ORIGINAL RESEARCH PAPER

Preparation, Optimization, and Characterization of CuInS$_2$ quantum dots by a D-optimal Design

Mahzad Mirzaie[1], Reza Khanbabaie*[2], Mohsen Jahanshahi[1], Ghasem Najafpour Darzi[3]

[1] *Faculty of Chemical Engineering, Nanotechnology Research Institute, Babol University of Technology, Babol, Iran*

[2] *Department of Physics, Faculty of Basic Sciences, Babol University of Technology, Babol, Iran*

[3] *Faculty of Chemical Engineering, Biotechnology Research Lab., Babol University of Technology, Babol, Iran*

ABSTRACT

Recently, safety concerns over the handling of nanomaterials have become an important issue. The aim of the present study was to optimize the key parameters in the hydrothermal synthesis of CuInS$_2$ quantum dots (QDs) as a non-toxic alternative to the cadmium-based QDs, that historically had dominated the literature. Response surface methodology (RSM) in combination with eliminate the D-optimal design was applied to optimize the synthesis and evaluate the Photoluminescence (PL) intensity as the response which is described by a reduced quadratic equation. The relationship between the PL intensity and independent variables (ligand/precursor, reaction time, reaction temperature, pH, and precursors ratio) was investigated using reduced quadratic polynomial equation. The produced QDs in the optimum condition were analyzed by UV-Vis, FESEM, and FTIR. The results showed that the nanoparticles have a high PL intensity and a red shift in both emission and absorption spectra which is a splendid point for their applications, especially in bioimaging. The interaction between variables was not significant and the temperature was the most effective variable of PL intensity. A good agreement between model predictedand experimental data confirmed the correlated model.

Keywords: *CuInS$_2$ QDs, Optimization, Response Surface Methodology, D-Optimal Design*

INTRODUCTION

As nanotechnology advances, nanosafety and the risks of toxicity and ecotoxicity associated with nanomaterials have become a matter of great concern due to their related contributions to the human health and the environment; since the nanomaterials could appear in air, water, soils, plants and consequently in human and animal bodies [1, 2].

QDs are inorganic semiconductor nanocrystals composed of a heavy-metal core and usually a shell, which have grasped a significant attention in recent years [3]. Their unique optical and electronic properties are captivating, leading to a variety of research and commercial applications including bioimaging, solar cells, LEDs, diode lasers, and transistors [4-7]. Until recently, cadmium-based QDs have been assuredly the most progressed, since the synthesis is straight-forward and their band gaps lie in the visible region of the spectrum, allowing for simple characterization. The inherent (eco)toxicity of these QDs has hindered their applicability, motivating researches into alternative, less toxic QDs [8-12]. I–III–VI CuInS$_2$ QDs are environmentally friendly and biocompatible which have emerged as particularly exciting materials for the synthesis of a new class of QDs, not only they contain no heavy metal ions, but also due to the unique structural and electronic properties that arise from the composition and structure of ternary

* Corresponding Author Email: *rkhanbabaie@nit.ac.ir*

semiconductor compounds in general [13, 14].

Various approaches have been reported for CuInS$_2$ syntheses such as solvothermal synthesis, single-source precursor routes and hot injection techniques which are based on organic solvents so their applications have been faced with several problems [15-18]. Direct hydrothermal synthesis of CuInS$_2$ QDs offers advantages such as lower reaction temperature with comparable photoluminescence quantum yield (PLQY), not using toxic and expensive organometallic reagents, does not need any surface functionalization during synthesis, no longer producing harmful bi-products, comparatively smaller particle size and tunable nanoparticles' size and morphology by controlling the precursors' concentration, temperature and time of reaction [19, 20].

There are few methods for direct hydrothermal synthesis of CuInS$_2$ QDs, while to tackle this problem, developing a proper synthesis method seems to be a necessity. According to an extensive survey on the literature, a very efficient facile direct synthesis method producing small size CuInS$_2$ QDs has been discovered in a work that Liu *et al.* do in order to prepare water-soluble high-quality ternary CuInS$_2$ QDs with mercaptopropionic acid (MPA) as the stabilizer by a novel hydrothermal synthesis route[8, 21, 22]. Many factors affect the CuInS$_2$ QDs synthesis such as reaction temperature, reaction time, precursors concentration ratio, pH and ligand/precursor concentration ratio. These parameters change the PL intensity and the size of CuInS$_2$ QDs. So it is necessary to optimize them for producing appropriate nanoparticles [19, 23, 24].

In order to achieve the optimum synthesis condition, previously one parameter has been changed while the others have been kept unchanged during the experiments. By this way, the influence of each parameter could be understood solely [25-30]. These traditional optimization methods have some disadvantageous. They require a considerable amount of work and time due to the high number of experiments. Also, the influence of parameters interaction couldn't be investigated [31]. In order to optimize the experimental synthesis conditions, multivariate statistical techniques can be employed. Among these optimization techniques, response surface methodology is the most popular tool in process optimization, consequently, the most applied [32]. Response surface methodology is a mathematical and statistical method that widely used for experiential modeling in order to evaluate

the influence of independent variables on dependent ones [33, 34]. Optimal designs initiate with a pseudo-random set of model points that enable the model fitting. The first choice can usually be upgraded by replacing a subset of the points with improved selections [35]. The optimal design uses several criteria to decide which replacements are suitable for the studied system, which the D-optimal algorithm is the most used criteria, which chooses runs that minimizes the determinant of the variance-covariance matrix [35].

To the best knowledge of authors, no study has been done on the optimization of the synthesis condition of CuInS$_2$ QDs using the response surface methodology approach. In a study, Pian Wu *et al.* optimized the formulation variables and process of acid-modified ZnSe/ZnS core/shell QDs using the response surface methodology [36]. In another study, Box–Behnken design (BBD) and response surface methodology were adopted to optimize the synthesis condition for ZnSe/ZnS core/shell QDs via microwave irradiation [37]. So, employing of RSM technique for CuInS$_2$ QDs synthesis condition can be considered as a new aspect of this work. At the present research, RSM coupled with D-optimal design was used to study the relationship between the independent (reaction time, reaction temperature, pH, precursors concentration ratio and ligand/precursor concentration ratio) and dependent (PL intensity and the desirable production output based on maximum PL intensity) variables in the optimized condition.

MATERIALS AND METHODS
Materials

All reagents were analytical grade and used directly without any purification. Copper(II) chloride dehydrate (CuCl$_2$.2H$_2$O), Indium(III) chloride tetrahydrate (InCl$_3$.4H$_2$O), Sulfourea (CS (NH$_2$)$_2$), Mercaptopropionic acid (MPA), and Sodium hydroxide (NaOH) were purchased from Sigma-Aldrich Corporation (St. Louis, MO, USA).

Synthesis of MPA-capped CuInS$_2$ QDs

The hydrothermal synthesis of hydrophilic MPA-capped CuInS$_2$ QDs was achieved by adopting a literature method in which the surfactant MPA acts not only as both stabilizing ligand and source of Sulphur for the nanoparticles but also as the reaction solvent [8, 22, 24]. The underlying principle behind this method is that excess of thiol promotes complete surface ligand coverage and therefore, good colloidal stability.

In this work, Indium(III) chloride and Copper(II) chloride dehydrate were used, because of their demonstrated reactivity and solubility. In a typical experiment, $CuCl_2.2H_2O$ (0.15 mmol) and $InCl_3.4H_2O$ (0.15 mmol) were dissolved in distilled water (10.5 ml). Then MPA (1.8 mmol) was injected into the solution, producing opaque yellow granules immediately. The pH value of the mixture solution was adjusted to 11.3 by the drop-wise addition of 2 mol/L NaOH solution with gentle magnetic stirring. During this process, the solution changed from turbid to clear pink (Fig. 1, step 3). After stirring for 10 min, CS $(NH_2)_2$ (0.30 mmol) was dissolved in the solution. The Cu–to–In–to–S and Cu–to–MPA precursor ratios were 1:1:2 and 1:12, respectively. All the above mentioned experimental procedures were performed at room temperature, and then the solution was transferred into a Teflon-lined stainless steel autoclave with a volume of 15 ml. The autoclave was maintained at 150℃ for 21 h after which cooled down to room temperature, quenching the reaction by a hydrocooling process. A purification method based on solvent extraction was used to separate unreacted precursors and reaction by-products from the as-synthesized hydrophilic QDs suspended in a nonorganic solvent. Ethanol was added to the solution to obtain $CuInS_2$ QDs precipitate, and the process was repeated three times. The unreacted residues were removed by the cycled washing. The $CuInS_2$ QDs was dried at 60 ℃ for 4–6 h (Fig. 1, step 5). The obtained powder was used for further measurements [8, 22, 24].

Characterization

Field emission Scanning electron microscopy (FESEM) experiments were performed on a TESCAN-Mira 3-XMU (Kohoutovice, Czech Republic) - operating at 3-30 KV voltage. FTIR spectra were recorded with a Beijing Rayleigh Analytical Instrument Corporation (Beijing, China). BRAIC-WQF-510 FTIR Spectrometer equipped with a DTGS detector (16 scans). UV-VIS absorption spectra of CIS QDs were obtained using UV-VIS spectrophotometer, LAMBDA™ 25, Wavelength range 190-1100 nm, PerkinElmer Co. (Waltham, MA., USA). The Photoluminescence spectra were measured by spectrofluorometer, Avaspec 2048 TEC, Avantes Co. (Apeldoorn, The Netherlands).

Design of experiment using response surface methodology and D-optimal approach

In order to perform a regression model, The Design Expert Software, version 10, based on RSM and D-optimal design was used. According to the primary studies, MPA/Cu (A), time (B), temperature (C), pH (D), and In/Cu (E) were selected as independent variables (Table 1) and PL intensity was chosen as the response to this research with the purpose of achieving the highest PL intensity which is desired in QDs applications.

The complete experimental runs and the corresponding responses are illustrated in Table 2.

The response behaviors can be defined using a quadratic polynomial model [38] by the following equation:

$$y = \beta_0 + \sum_{i=1}^{k} \beta_i x_i + \sum_{i=1}^{k} \beta_{ii} x_i^2 + \sum_{i=1 \leq i \leq j}^{k} \beta_{ij} x_i x_j + \varepsilon \tag{1}$$

Where y is the response (dependent variable),
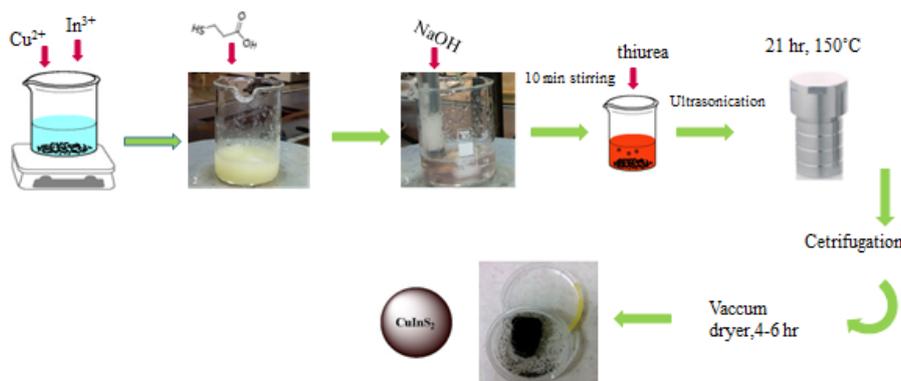
Fig. 1. MPA-capped $CuInS_2$ synthesis steps

J. Water Environ. Nanotechnol., 3(4): 311-320 Autumn 2018

313

x_i and x_j are independent variables, ε is the residual, β_0 is the constant coefficient, β_i, β_{ii} and β_{ij} are the coefficients for the linear, quadratic, and the interaction terms, respectively [39].

RESULTS AND DISCUSSION

Response surface methodology and D-optimal approach

The PL intensity response can be described by a reduced quadratic equation based on coded factors as follow:

$$\text{PL intensity} = -0.020 + 0.16\,A + 0.098\,B + 0.73\,C + 0.39\,D + 0.12\,E - 0.25\,A^2 + 0.55\,C^2 + 0.16\,E^2 \quad (2)$$

The interaction and some quadratic coefficients of PL intensity model were insignificant and excluded from the model. The equation demonstrated that

the PL intensity model was sensitive to all factors. Model assessment was done by the coefficient of determination (R-squared). According to (Fig. 2), the R-squared value of 0.9201 for PL intensity and model shows that 92.01% of the variability is matched by the experimental data (Fig. 2), which a reasonable agreement between predicted and actual values is understood.

The analysis of variance (ANOVA) was applied to verify the model accuracy [33, 40]. The ANOVA for the predicted model is listed in Table 3.

The model significance can be described using the p-value and F value, which the smaller p-value (<0.1) and larger F value show the more significant model coefficient [34, 41]. As shown in Table 3, the F-value of 20.14 for PL intensity confirms that the model is highly significant. In addition, the model

Table 1. The dependent and independent variables

Variables				
Factors	Name	Units	Minimum	Maximum
A	MPA/Cu		10 (-1)	18 (+1)
B	Time	hr	17(-1)	25(+1)
C	Temperature	°C	120(-1)	160(+1)
D	pH		8(-1)	12(+1)
E	In/Cu		1(-1)	5(+1)

Response				
Response	Name	Units	Minimum	Maximum
R1	PL intensity	a.u.	0.014	1

Table 2. The design table of experiments and response values

Run	A: MPA/Cu	B: Time hr	C: Temp °C	D:pH	E: In/Cu	PL intensity
1	10	21	150	11.3	1	0.42
2	12	21	150	11.3	1	0.93
3	14	21	150	11.3	1	0.9
4	15	21	150	11.3	1	0.89
5	16	21	150	11.3	1	0.88
6	18	21	150	11.3	1	0.78
7	12	17	150	11.3	1	0.49
8	12	19	150	11.3	1	0.67
9	12	21	150	11.3	1	0.9
10	12	23	150	11.3	1	0.95
11	12	25	150	11.3	1	0.83
12	12	21	120	11.3	1	0.071
13	12	21	130	11.3	1	0.16
14	12	21	140	11.3	1	0.31
15	12	21	150	11.3	1	0.91
16	12	21	160	11.3	1	0.47
17	12	21	150	8	1	0.1
18	12	21	150	9	1	0.14
19	12	21	150	10	1	0.45
20	12	21	150	11	1	0.87
21	12	21	150	12	1	0.62
22	12	21	150	11.3	1	0.9
23	12	21	150	11.3	2	0.96
24	12	21	150	11.3	3	0.98
25	12	21	150	11.3	4	0.99
26	12	21	150	11.3	5	0.89

adequacy was further verified by the p-value less than 0.0001.

The influence of replicate points and errors dependence of model can be surveyed using the lack of fit test [33, 40]. As insignificant lack of fit is necessary, the model fitting was confirmed by the p-values of 0.8097 for PL intensity [42].

Moreover, the adequacy of the model is also should be studied using plots of normal probability and residuals vs. predicted [33, 38, 40] (Fig. 3). As shown in (Fig. 3), as expected the straight line of residual points on the normal probability plot for PL intensity (Fig. 3a) is revealed, confirming the normal distribution of errors [38, 40]. In addition,
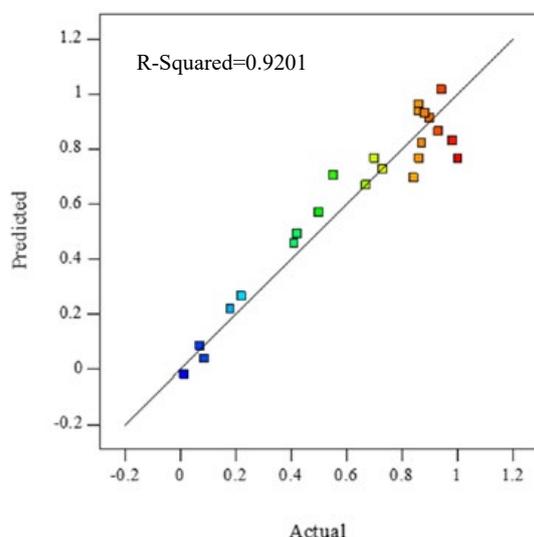
Fig. 2. The actual vs. predicted data for PL intensity

the assumption of constant variance is tested by residual versus the predicted responses. The plot should be a random scatter, which observed for PL intensity (Fig. 3b) [38].

The perturbation plots of the PL intensity as a response is shown in (Fig. 4). This plot helps to compare the impacts of all the factors at a particular point in the design space, which the response is plotted by changing only one factor over its range at a constant value of other factors [43]. As shown in (Fig. 4) the most effective parameters on PL intensity was temperature, while the other factors were less sensitive to PL intensity. As the reaction temperature increases the PL intensity increases due to better ligand passivation, while it has been decreased severely at higher temperatures. This phenomenon happens because of the pyrolysis of MPA and poor ligand passivation. [19] Increase of nanoparticles size resulting in agglomeration is another reason for the reduction in PL intensity [44, 28].

The 3D plots at (Fig. 5) show the simultaneous effect of temperature (as the most important parameter) and the other factors on PL intensity, which increased significantly by temperature enhancement. A linear and nonlinear growing trend in PL intensity was observed by increasing pH (Fig. 5c) and MPA/Cu (Fig. 5a) while the time and In/Cu did not show a considerable effect on PL intensity (Fig. 5b and d). MPA/ Cu and pH can affect the decomposition of Cu-In-MPA complex. In the low concentration of MPA as the temperature and pH increases, PL intensity of

Table 3. ANOVA for PL intensity response

Source	Sum of Squares	Df	Mean Square	F-Value	p-value Prob > F
PL intensity	2.15	8	0.27	20.14	< 0.0001
A-MPA/Cu	0.093	1	0.093	6.96	0.0195
B-Time	0.096	1	0.096	7.21	0.0178
C-Temperature	0.81	1	0.81	60.50	< 0.0001
D-pH	0.79	1	0.79	59.64	< 0.0001
E- In/Cu	0.065	1	0.065	4.90	0.0439
A^2	0.073	1	0.073	5.48	0.0346
B^2	0.098	1	0.098	7.36	0.0168
C^2	0.033	1	0.033	2.49	0.1368
Residual	0.19	14	0.013		
Lack of Fit	0.14	12	0.012	0.52	0.8097
Pure Error	0.045	2	0.023		
Cor Total	2.33	22			

Table 4. Result of model verification at an optimum combination

Run	MPA/Cu	Time	Temp	pH	In/Cu	Predicted PL intensity	Experimental PL intensity
27	12.6	21.46	152.00	11.15	3.5	0.99	0.94
				Without variable constrains			

J. Water Environ. Nanotechnol., 3(4): 311-320 Autumn 2018

315
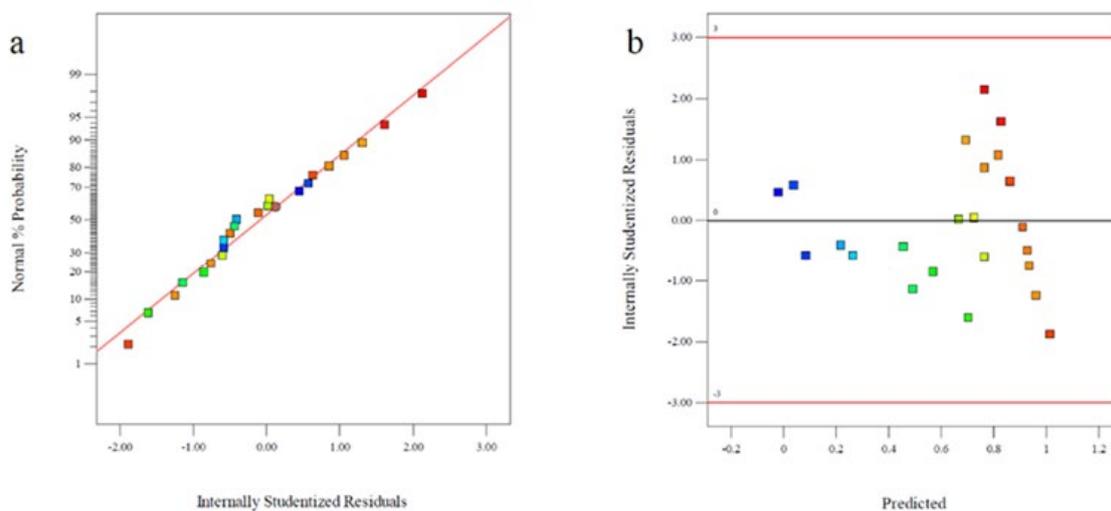
Fig. 3. Normal probability plot of residuals (a) and internally studentized residual versus the predicted plot (b) for PL intensity

Deviation from Reference Point (Coded Units)
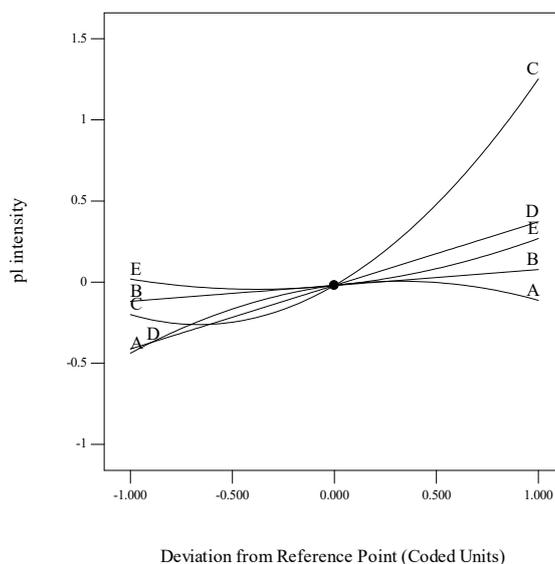
Fig. 4. Perturbation plots of pl intensity

nanoparticles decreases due to the formation of $Cu(OH)_2$ precipitates. Excess MPA/Cu distort the surface to form new non-radiative defects which quench the PL intensity of as-prepared QDs [19]. Shortage of surface ligands causes instability and agglomeration of QDs resulted in diminishing PL intensity.

Model verification and optimization

As the maximum values of PL intensity were crucial for optimal condition, the multi-response optimization was applied using desirability function. Table 4 shows optimized

new experimental test as optimum run without constrains. The result verified that the experimental data and predicted values were in good agreement and the relative error was around 5%, confirming that the model had enough accuracy to predict removal percentage for this system.

Preparation of CuInS₂ QDs under the optimum condition

Structural characterization: The surface structural analysis of the as-synthesized CuInS₂ QDs were undertaken using FESEM and FTIR. FESEM observation for CuInS₂ nanoparticles

produced under the optimum condition is shown in (Fig. 6). By analysis of the FESEM image, we determined the particle size of most of CuInS$_2$ QDs obtained was approximately 7 nm.

Because of their small dimensions, QDs have an inherently large surface to volume ratio, therefore, surface properties play a crucial role in their conjugation and also photoluminescence
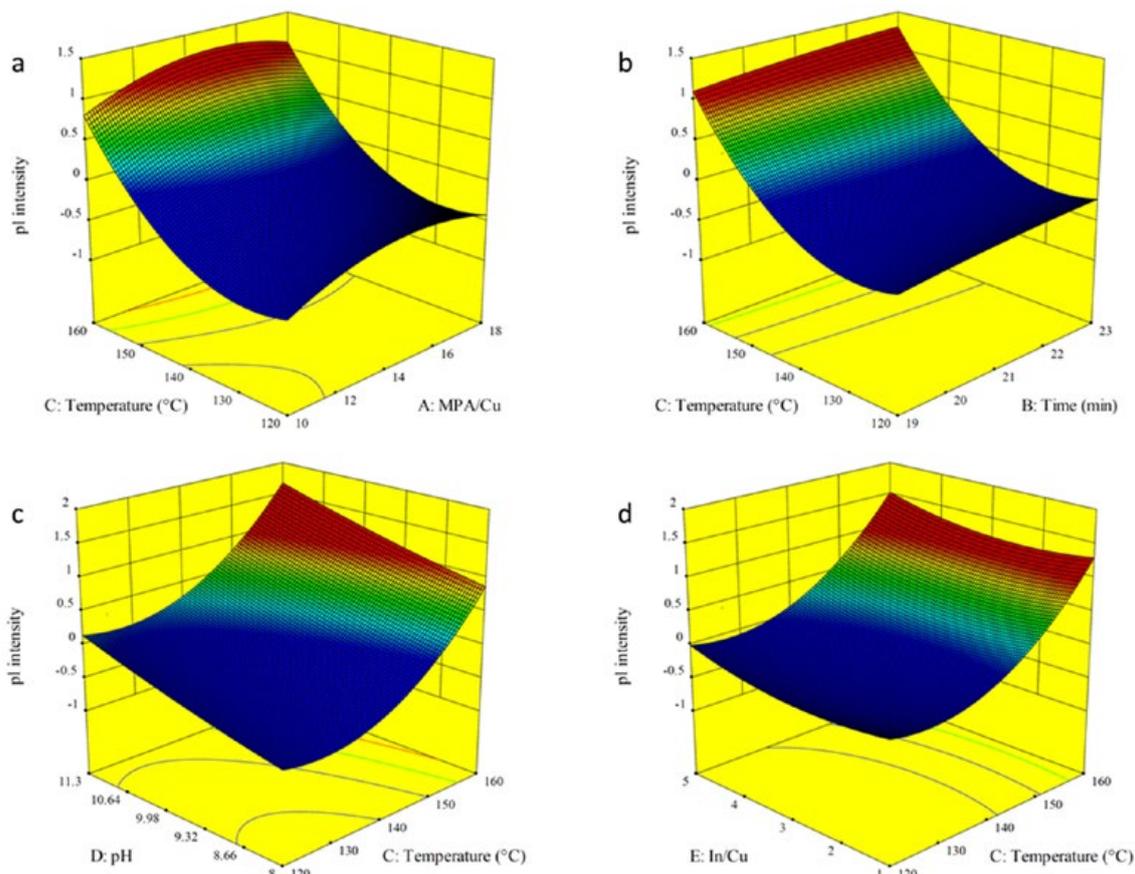
Fig. 5. 3D response surface plots of PL intensity as a function of (a) temperature and MPA/Cu (b) temperature and time, (c) temperature and pH (d) temperature and In/Cu at constant values of other variables
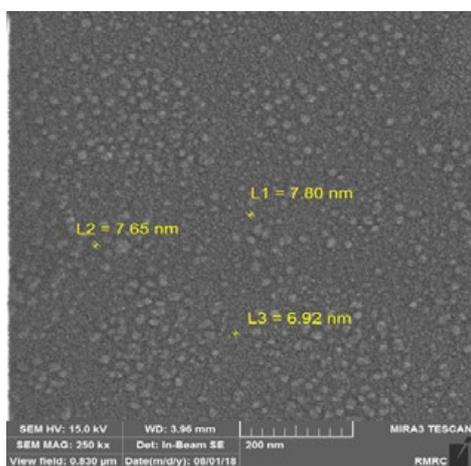
Fig. 6. FESEM image of MPA-capped CuInS$_2$ QDs
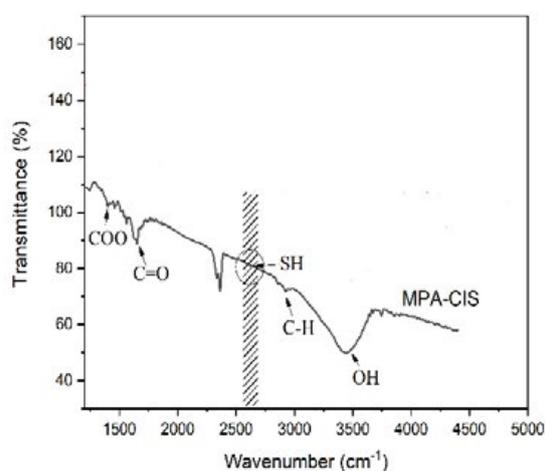
Fig. 7. FTIR analysis of MPA-capped CuInS$_2$ QDs

J. Water Environ. Nanotechnol., 3(4): 311-320 Autumn 2018

317
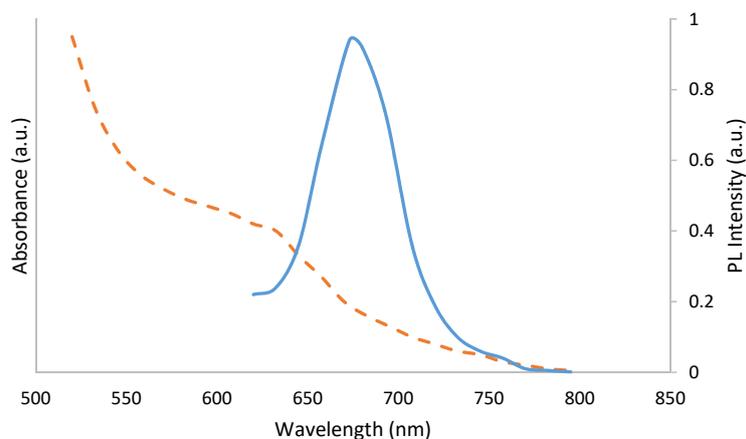
Fig. 8. a: Fluorescence emission spectra (solid line) b: UV/Vis absorption spectra (dashed line) for as-synthesized CuInS$_2$ QDs

properties. As such, it is important to investigate the functionalization of the surface, determining the extent of surface coverage, the nature of the capping ligands, including their tendency to associate with surface atoms and surface defects [44-47]. To further characterize the as-synthesized CuInS$_2$ QDs, FTIR has been carried out (Fig. 7).

The FTIR spectra pointed that most functional groups of the as-synthesized QDs could be clearly found through the characteristic peaks of O–H (3448 cm^{-1} stretching vibration), –COOH (2370 cm^{-1} asymmetric stretching vibration), C=O (1705 cm^{-1} stretching vibration), C-O (1480 cm^{-1} stretching vibration). The absence of the characteristic peak of S– H between 2550 to 2680 cm^{-1} indicated that the final CuInS$_2$ nanoparticles contain MPA on their surface, which might be caused by the covalent bonds between thiols and metal atoms [19, 24] of the ternary QDs.

Optical Characterization: The emissive properties of CuInS$_2$ QDs were explored with fluorescence spectroscopy; a typical PL spectrum for CuInS$_2$ QDs under the optimum condition is shown in (Fig. 8a). It can be seen that the nanoparticles exhibit excellent fluorescence emission spectra with the emission peak around 675 nm. As obvious red shift of emission for as-synthesized QDs at the optimum condition compared to the synthesis in other conditions is clear. The redshift of emission peak demonstrates that the nanoparticles are in the near infrared region which is more suitable for biological imaging and detection [23]. The emission band is narrow and symmetrical. A typical absorption spectrum is also shown in (Fig. 8b); The UV-VIS absorption spectra of the as-prepared CuInS$_2$ QDs have been measured at room temperature.

CONCLUSION

At the present research, CuInS$_2$ quantum dots have been successfully synthesized by hydrothermal method. The influence of independent variables including MPA/Cu, time, temperature, pH, and In/Cu on the PL intensity as a response was studied using RSM and D-optimal design and the optimum condition for producing nanoparticles with high PL intensity was achieved. UV-VIS, FESEM, and FTIR analysis on the produced QDs in the optimum condition showed the nanoparticles have a near-infrared narrow PL spectra with high PL intensity. A reduced quadratic equation has been proposed to describe PL intensity. The statistical analysis and reduced quadratic models showed that the temperature variables were the most effective parameters of PL intensity. A good agreement between the predicted results and the experimental data was observed in model analysis and optimization step.

CONFLICT OF INTEREST

The authors declare that there are no conflicts of interest regarding the publication of this manuscript.

REFERENCES

1. CHUANKRERKKUL, N. and SANGSUK, S. 2008. *Current Status of Nanotechnology Consumer Products and Nano-Safety Issues.*

2. George S, Ho SS, Wong ESP, Tan TTY, Verma NK, Aitken RJ, et al. The multi-facets of sustainable nanotechnology – Lessons from a nanosafety symposium. Nanotoxicology. 2015;9(3):404-6.

3. Reimann SM, Manninen M. Electronic structure of quantum dots. Reviews of Modern Physics. 2002;74(4):1283-342.

4. AL-AHMADI, A. 2012. *Quantum Dots: a variety of new applications*, InTech.

5. Bera D, Qian L, Tseng T-K, Holloway PH. Quantum Dots and Their Multimodal Applications: A Review. Materials. 2010;3(4):2260-345.

6. Azzazy HME, Mansour MMH, Kazmierczak SC. From diagnostics to therapy: Prospects of quantum dots. Clinical Biochemistry. 2007;40(13-14):917-27.

7. Gao X, Cui Y, Levenson RM, Chung LWK, Nie S. In vivo cancer targeting and imaging with semiconductor quantum dots. Nature Biotechnology. 2004;22(8):969-76.

8. MIRZAEI M., J. M., KHANBABAIE R., NAJAFPOUR G.,2017. Nanotechnology and Neuroscience Convergence: A Novel Tool forNeurotransmitters Monitoring. *International Journal of Engineering* 30(2)**,** 10.

9. Michalet X, Pinaud F, Lacoste TD, Dahan M, Bruchez MP, Alivisatos AP, et al. Properties of Fluorescent Semiconductor Nanocrystals and their Application to Biological Labeling. Single Molecules. 2001;2(4):261-76.

10. Rzigalinski BA, Strobl JS. Cadmium-containing nanoparticles: Perspectives on pharmacology and toxicology of quantum dots . Toxicology and Applied Pharmacology. 2009;238(3):280-8.

11. AZZAZY, H. M., MANSOUR, M. M. and KAZMIERCZAK, S. C.,2006. Nanodiagnostics: a new frontier for clinical laboratory medicine. *Clin Chem,* 52(7), 1238-46.

12. Hardman R. A Toxicologic Review of Quantum Dots: Toxicity Depends on Physicochemical and Environmental Factors. Environmental Health Perspectives. 2006;114(2):165-72.

13. Kim Ys, Lee Y, Kim Y, Kim D, Choi HS, Park JC, et al. Synthesis of efficient near-infrared-emitting CuInS2/ZnS quantum dots by inhibiting cation-exchange for bio application. RSC Advances. 2017;7(18):10675-82.

14. Foda MF, Huang L, Shao F, Han H-Y. Biocompatible and Highly Luminescent Near-Infrared CuInS2/ZnS Quantum Dots Embedded Silica Beads for Cancer Cell Imaging. ACS Applied Materials & Interfaces. 2014;6(3):2011-7.

15. AL-AHMADI, A. 2012. *State-of-the-Art of Quantum Dot System Fabrications*, InTech.

16. Shei S-C, Chiang W-J, Chang S-J. Synthesis of CuInS2 quantum dots using polyetheramine as solvent. Nanoscale Research Letters. 2015;10(1).

17. Zhong H, Lo SS, Mirkovic T, Li Y, Ding Y, Li Y, et al. Noninjection Gram-Scale Synthesis of Monodisperse Pyramidal CuInS2 Nanocrystals and Their Size-Dependent Properties. ACS Nano. 2010;4(9):5253-62.

18. Karakoti AS, Shukla R, Shanker R, Singh S. Surface functionalization of quantum dots for biological applications. Advances in Colloid and Interface Science. 2015;215:28-45.

19. Arshad A, Chen H, Bai X, Xu S, Wang L. One-Pot Aqueous Synthesis of Highly Biocompatible Near Infrared CuInS2Quantum Dots for Target Cell Imaging. Chinese Journal of Chemistry. 2016;34(6):576-82.

20. Sun C, Gardner JS, Shurdha E, Margulieux KR, Westover RD, Lau L, et al. A High-Yield Synthesis of Chalcopyrite CuInS2Nanoparticles with Exceptional Size Control. Journal of Nanomaterials. 2009;2009:1-7.

21. Liu S, Shi F, Chen L, Su X. Dopamine functionalized CuInS2 quantum dots as a fluorescence probe for urea. Sensors and Actuators B: Chemical. 2014;191:246-51.

22. Lin Z, Fei X, Ma Q, Gao X, Su X. CuInS2quantum dots@ silica near-infrared fluorescent nanoprobe for cell imaging. New J Chem. 2014;38(1):90-6.

23. Protière M, Nerambourg N, Renard O, Reiss P. Rational design of the gram-scale synthesis of nearly monodisperse semiconductor nanocrystals. Nanoscale Research Letters. 2011;6(1):472.

24. Liu S, Zhang H, Qiao Y, Su X. One-pot synthesis of ternary CuInS2quantum dots with near-infrared fluorescence in aqueous solution. RSC Adv. 2012;2(3):819-25.

25. Hua J, Du Y, Wei Q, Yuan X, Wang J, Zhao J, et al. Composition-dependent photoluminescence properties of CuInS2/ZnS core/shell quantum dots. Physica B: Condensed Matter. 2016;491:46-50.

26. Jara DH, Stamplecoskie KG, Kamat PV. Two Distinct Transitions in CuxInS2 Quantum Dots. Bandgap versus Sub-Bandgap Excitations in Copper-Deficient Structures. The Journal of Physical Chemistry Letters. 2016;7(8):1452-9.

27. Chen Y, Li S, Huang L, Pan D. Green and Facile Synthesis of Water-Soluble Cu–In–S/ZnS Core/Shell Quantum Dots. Inorganic Chemistry. 2013;52(14):7819-21.

28. Li D, Zou Y, Yang D. Controlled synthesis of luminescent CuInS2 nanocrystals and their optical properties. Journal of Luminescence. 2012;132(2):313-7.

29. Almendral-Parra M-J, Alonso-Mateos Á, Sánchez-Paradinas S, Boyero-Benito JF, Rodríguez-Fernández E, Criado-Talavera JJ. Procedures for Controlling the Size, Structure and Optical Properties of CdS Quantum Dots during Synthesis in Aqueous Solution. Journal of Fluorescence. 2011;22(1):59-69.

30. Deng D, Chen Y, Cao J, Tian J, Qian Z, Achilefu S, et al. High-Quality CuInS2/ZnS Quantum Dots for In vitro and In vivo Bioimaging. Chemistry of Materials. 2012;24(15):3029-37.

31. ASHASSI-SORKHABI, H., REZAEI-MOGHADAM, B., BAGHERI, R., ABDOLI, L. and ASGHARI, E.,2015. Synthesis of Au Nanoparticles by Thermal, Sonochemical and Electrochemical Methods: Optimization and Characterization. *Physical Chemistry Research,* 3(1)**,** 24-34.

32. Khalili S, Khoshandam B, Jahanshahi M. Optimization of production conditions for synthesis of chemically activated carbon produced from pine cone using response surface methodology for CO2 adsorption. RSC Advances. 2015;5(114):94115-29.

33. Bezerra MA, Santelli RE, Oliveira EP, Villar LS, Escaleira LA. Response surface methodology (RSM) as a tool for optimization in analytical chemistry. Talanta. 2008;76(5):965-77.

34. Khakpour H, Haghgoo M, Etemadi K. Analysis and optimization of viscosity of concentrated silica suspensions by response surface methodology (RSM): Control of particle modality. Journal of Dispersion Science and Technology. 2017;39(9):1352-9.

35. Goos P, Jones B. Optimal Design of Experiments. John Wiley & Sons, Ltd; 2011.

J. Water Environ. Nanotechnol., 3(4): 311-320 Autumn 2018

319

36. Wu P, Huang R, Li G, He Y, Chen C, Xiao W, et al. Optimization of Synthesis and Modification of ZnSe/ZnS Quantum Dots for Fluorescence Detection of Escherichia coil. Journal of Nanoscience and Nanotechnology. 2018;18(5):3654-9.

37. Ma R, Zhou P-J, Zhan H-J, Chen C, He Y-N. Optimization of microwave-assisted synthesis of high-quality ZnSe/ZnS core/shell quantum dots using response surface methodology. Optics Communications. 2013;291:476-81.

38. Vera Candioti L, De Zan MM, Cámara MS, Goicoechea HC. Experimental design and multiple response optimization. Using the desirability function in analytical methods development. Talanta. 2014;124:123-38.

39. MYERS, R. H., D.C. MONTGOMERY, AND C.M. ANDERSON-COOK 2016. *Response surface methodology: process and product optimization using designed experiment*, John Wiley & Sons.

40. Chieng BW, Ibrahim NA, Yunus WMZW. Optimization of Tensile Strength of Poly(Lactic Acid)/Graphene Nanocomposites Using Response Surface Methodology. Polymer-Plastics Technology and Engineering. 2012;51(8):791-9.

41. Horchani H, Chaâbouni M, Gargouri Y, Sayari A. Solvent-free lipase-catalyzed synthesis of long-chain starch esters using microwave heating: Optimization by response surface methodology. Carbohydrate Polymers. 2010;79(2):466-74.

42. Witek-Krowiak A, Chojnacka K, Podstawczyk D, Dawiec A, Pokomeda K. Application of response surface methodology and artificial neural network methods in modelling and optimization of biosorption process. Bioresource Technology. 2014;160:150-60.

43. Lucas JM. Response Surface Methodology: Process and Product Optimization Using Designed Experiments, 3rd edition. Journal of Quality Technology. 2010;42(2):228-30.

44. Liu S, Pang S, Huang H, Su X. 3-Aminophenylboronic acid-functionalized CuInS2quantum dots as a near-infrared fluorescence probe for the detection of dicyandiamide. The Analyst. 2014;139(22):5852-7.

45. Lin Z, Ma Q, Fei X, Zhang H, Su X. A novel aptamer functionalized CuInS2 quantum dots probe for daunorubicin sensing and near infrared imaging of prostate cancer cells. Analytica Chimica Acta. 2014;818:54-60.

46. Yue W, Wang M, Nie G. Ternary MEH-PPV-CuInS2/ZnO solar cells with tunable CuInS2 content. Solar Energy. 2014;99:126-33.

47. Peng Z, Liu Y, Shu W, Chen K, Chen W. Efficiency enhancement of CuInS2 quantum dot sensitized TiO2 photo-anodes for solar cell applications. Chemical Physics Letters. 2013;586:85-90.